Available online at www.sciencedirect.com
ScienceDirect
Progress in Natural Science 19 (2009) 187–193
Progress in Natural Science
www.elsevier.com/locate/pnsc

A modeling study of relation between cloud amount and SST over Western Tropical Pacific cloudy regions during TOGA COARE

Shouting Gao [a,*], Xiaopeng Cui [a], Xiaofan Li [b]

[a] *Laboratory of Cloud-Precipitation Physics and Severe Storms (LACS), Institute of Atmospheric Physics, Chinese Academy of Sciences, Beijing 100029, China*
[b] *Joint Center for Satellite Data Assimilation and NOAA/NESDIS/Center for Satellite Applications and Research, Camp Springs, MD, USA*

Received 20 March 2008; received in revised form 18 June 2008; accepted 22 July 2008

Abstract

The relationship between cloud amount and sea surface temperature (SST) over Western Tropical Pacific cloudy regions during TOGA COARE is investigated based on hourly grid simulation data from a two-dimensional coupled ocean–cloud resolving atmosphere model. The model is forced by the large-scale vertical velocity and zonal wind observed and derived from TOGA COARE for a 50-day period. The cloud amount becomes smaller when the ocean surface gets warmer, which is similar to previous relations obtained from observational analyses. As SST increases, the atmospheric temperature increases whereas the surface sensible heat flux decreases. The atmospheric water vapor is not sensitive to SST whereas the surface evaporation flux decreases as SST increases. These indicate that the oceanic effects do not play an important role in determining atmospheric heat and water vapor budgets. The cold atmosphere produces a larger amount of ice clouds that cover a larger area than the warm atmosphere does. The large amounts of ice clouds lead to cooling of the ocean surface through reflecting large amount of solar radiation back to the space. Thus, the negative correlation between the cloud amount and SST only accounts for the important atmospheric effects on the ocean.

Keywords: Cloud amount; Sea surface temperature; Coupled ocean–cloud resolving atmosphere model; TOGA COARE

1. Introduction

Clouds are an important regulator for tropical atmosphere and ocean as they affect atmospheric heat, moisture and momentum structures through changing cloud microphysical, thermodynamic and mixing processes, and they affect the upper ocean thermal structures through changing solar radiative inputs. For the planetary scale, the development of convection is associated with upward motion over western Pacific warm pool, which is surrounded by the downward motion over eastern Pacific cold tongue. Over the warm pool, where the area-mean sea surface temperature (SST) is usually 3–5 °C warmer than the SST over the cold tongue, the SST shows the diurnal variations with the maximum difference of 1–3 °C, and experiences the warming in the clear-sky conditions and the cooling in the westerly wind burst as observed during the Tropical Ocean Global Atmosphere Coupled Ocean–Atmosphere Response Experiment (TOGA COARE) [1–3].

Observational analysis and numerical modeling studies have revealed the relationship between the cloud amount and SST [4–7]. Ramanathan and Collins [8] reported that cloud cover associated with upper tropospheric anvil clouds increases with the SST. Arking and Ziskin [9] analyzed the relation between the Earth Radiation Budget Experiment (ERBE) radiance and SST, and they found that clouds are affected by SST but not vice versa. Bony et al. [10] analyzed the relation between cloud fraction and SST during the period of 1987–1988 using cloud

* Corresponding author. Tel.: +86 10 82995307; fax: +86 10 82995308.
E-mail address: gst@lasg.iap.ac.cn (S. Gao).

1002-0071/$ - see front matter © 2008 National Natural Science Foundation of China and Chinese Academy of Sciences. Published by Elsevier Limited and Science in China Press. All rights reserved.
doi:10.1016/j.pnsc.2008.07.006

fraction data from the International Satellite Cloud Climatology Project (ISCCP) C2 dataset [11], the Tiros Operational Vertical Sounder (TOVS) Pathfinder Path A dataset from Goddard Laboratory for Atmospheres [12] and SST data from National Center for Environmental Prediction (NCEP) [13]. They found that cloud fraction decreased when SST increased from 20 to 26 °C, but the relation between cloud fraction and SST above 26 °C depended on the regime. Tompkins and Craig [14] carried out a three-dimensional cloud-resolving modeling study to examine sensitivity of tropical convection to SST in the absence of large-scale flow and found that cloud fraction decreased from 17% to 15% as SST increased from 25 to 29 °C. Wu and Moncrieff [15] conducted two-dimensional cloud-resolving model simulations with a 39-day mean forcing during TOGA COARE, and their analysis on equilibrium simulation data showed that cloud fraction was reduced from 71% to 63% as SST increased from 27.37 to 31.37 °C. Costa et al. [16] studied the sensitivity of cloud fraction to the change of SST with a two-dimensional cloud-resolving model during TOGA COARE and revealed that the increase of SST led to an increase of cloud fraction in the upper troposphere, while the decrease of SST caused an increase of cloud fraction in the lower troposphere and a decrease of cloud fraction in the upper troposphere. Lindzen et al. [17] analyzed the daily cloud data from Japanese Geostationary Meteorological Satellite-5 and weekly mean SST data from NCEP [13] over the warm pool region (30°S–30°N, 130°–170°W). They found that the area of cloud coverage decreased with increasing SST over the cloudy region.

The above sensitivity experiments of SST with cloud-resolving models have evident flaws that SST was horizontally uniform in the model domain, and the atmospheric effects on ocean were not allowed. In fact, the coupled ocean–cloud resolving atmosphere model simulation [18,19] showed that SST is not horizontally uniform and its change is associated with precipitation. In this study, the relation between cloud amount and SST over cloudy regions is revisited by analyzing a coupled ocean–cloud resolving atmosphere model simulation with the forcing from TOGA COARE to answer the questions of that what is the relation between cloud amount and SST, and that if the relation can explain both atmospheric effects on the ocean and oceanic effects on the atmosphere.

2. Model description and experiment design

The 50-day simulation data from two-dimensional (2D) coupled ocean–cloud resolving atmosphere model simulation carried out by Gao et al. [19] were analyzed in this study. The coupled model was originally developed by Li et al. [18] by coupling a 2D cloud-resolving model with a 2D embedded mixed-layer ocean circulation model. The coupled model with cyclic lateral boundaries uses a horizontal domain of 768 km, a horizontal grid resolution of 1.5 km, and a time step of 12 s.

The cloud-resolving model was developed by Soong and Ogura [20], Soong and Tao [21], and Tao and Simpson [22] and modified by Li et al. [23]. The cloud model includes five prognostic equations for mixing ratios of cloud water, raindrops, cloud ice, snow and graupel, respectively. It also includes the cloud microphysical parameterization schemes [24–28], and interactive solar and thermal infrared radiation parameterization schemes [29–31]. At the top (42 hPa) of the model, a free-slip condition is used for horizontal winds, temperature, and specific humidity, whereas zero vertical velocity is applied [22]. The vertical grid resolution ranges from about 200 m near the surface to about 1 km near 100 hPa.

The embedded mixed-layer ocean circulation model was originally developed by Adamec et al. [32], and modified by Sui et al. [2] with a Kraus-Turner mixing scheme [33]. The 2D embedded mixed-layer ocean circulation model consists of an ocean mixed-layer model and an ocean circulation model including advections, in which the models communicate to each other through the embedded technique developed by Adamec et al. [32]. The vertical grid resolution ranges from about 1 m near the ocean surface to about 50 m near the lower levels in the ocean model. The depth of the ocean model is 500 m. The vertical distribution of solar radiation ($I = I_o[re^{-\gamma_1 z} + (1-r)e^{-\gamma_2 z}]$) is defined by setting $r = 0.77$, $\gamma_1^{-1} = 0.65$ m, and $\gamma_2^{-1} = 14$ m [34], where I_o is the solar radiation at the ocean surface, r is an attenuation parameter; γ_1^{-1} and γ_2^{-1} are attenuation lengths for solar radiation penetration, and z is positive downward with $z = 0$ being the ocean surface. The ocean model is coupled with the above cloud-resolving model through surface momentum, radiative, heat, and fresh water fluxes.

Only the cloud-resolving model is forced by zonally uniform vertical velocity and zonal wind, which is derived by Sui et al. [35]. Fig. 1 shows the time evolution of vertical distribution of the large-scale atmospheric vertical velocity and zonal wind during 11 November 1992–1 January 1993 that are imposed in the model. The model is integrated from 1000 LST 11 November 1992 to 1600 LST 1 January 1993 (a total of 50.25 days). Gao et al. [19] conducted a comparison study between model simulations and observations in terms of mixed-layer temperature and surface rain rate. The simulated mixed-layer temperature generally follows the observed SST, but the observed SST (~2 to 3 °C) is larger than the simulated SST (~1 °C) in late November to early December 1992. The coupled model has the same capability to simulate zonal-mean SST as does the one-dimensional ocean mixed-layer model with COARE-derived surface forcing [3]. They found that SST was warmer than 29.5 °C over the areas with the absence of rainfall, whereas it was colder than 29 °C over the rainfall areas, indicating that the coupled model is capable of simulating the air–sea coupling processes. The simulated hourly surface rain rates generally follow the observations as indicated by their linear correlation coefficient of 0.55, which is statistically significant. But the simulated amplitudes are generally larger than the observed amplitudes

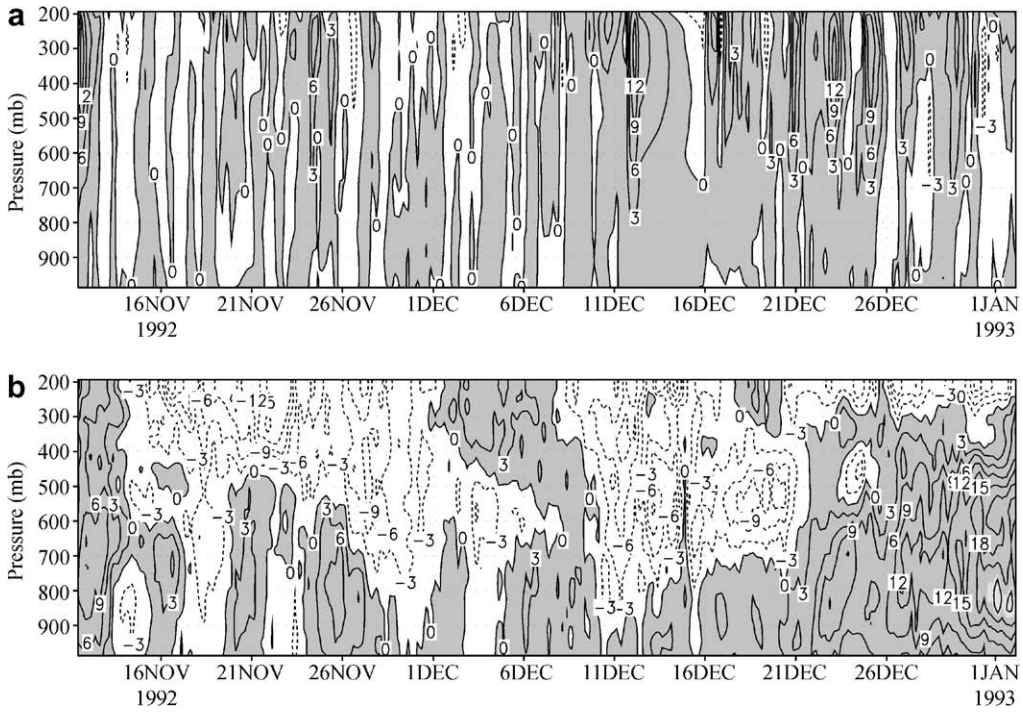

Fig. 1. Time evolution of (a) vertical velocity (cm s^{-1}) and (b) zonal wind (m s^{-1}) observed and derived during TOGA COARE for a 50-day period. Upward motion in (a) and westerly winds in (b) are shaded.

and there are some phase differences, which may be partly due to an inconsistency between the imposed vertical velocity and the observed rain rate. Detailed comparisons between simulations and observations can be found in [36].

3. Results

In this study, the grid with the sum of ice-water path (IWP: sum of mass-integrated mixing ratios of cloud ice, snow and graupel) and liquid water path (LWP: sum of mass-integrated mixing ratios of cloud water and rainwater) of larger than 0.005 mm was considered as cloudy. The SST and other quantities averaged over cloudy regions were calculated by dividing the summation of these quantities at cloudy grids by the number of cloudy grids. In the following discussions, all the quantities shown are those averaged over cloudy regions using hourly grid data with a 1.5 km horizontal resolution. The time-mean cloud amount is 62.2%, which is similar to the cloud amount calculated from ISCCP dataset (55–65%) [10]. The cloud amount decreases with increasing SST (Fig. 2). The negative correlation between cloud amount and SST is similar to the previous numerical and observational studies. The correlation coefficient is −0.21. Student's *t*-test on the significance of the correlation coefficients is conducted using 1240 degrees of freedom and a critical correlation coefficient at the 1% significant level is 0.07. Thus, the correlation is statistically significant. Fig. 2 shows two basic regimes: The cloud amount is mostly larger than 40% when SST is at 28–29 °C, whereas it is from 0 to 100% when SST is at 29–30 °C. The mean cloud amounts are 85.6% when

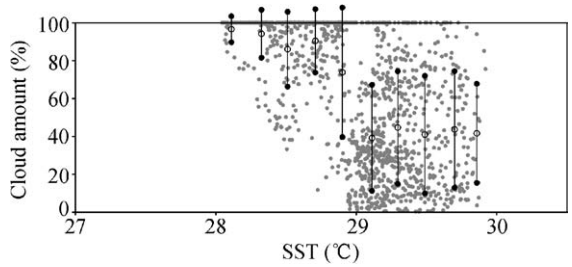

Fig. 2. Scatterplot of cloud amount (%) versus SST (grey) and against SST binned at 0.2 °C intervals. The error bars indicate the standard deviations within each SST category.

SST is at 28–29°C and 41.8% when SST is at 29–30 °C (Table 1).

Clouds can be categorized into convective, raining stratiform, and non-raining stratiform clouds using the partition method developed by Sui et al. [37]. In this newly developed cloud partition method, the rainfall is considered as convective when IWP/LWP is smaller than 0.2 and IWP is larger than the sum of its mean and standard deviation (2.55 mm). This convective-stratiform rainfall partition is similar to that developed by Tao et al. [38], which was further modified by Sui et al. [39] The convective, raining stratiform, and non-raining stratiform cloud amounts as functions of SST are shown in Fig. 3. Convective, raining stratiform, and non-raining stratiform cloud amounts generally decrease as SST increases. The root-mean-square (RMS) differences between cloud amount and convective cloud amount, between cloud amount and raining stratiform cloud amount, and between cloud

Table 1
Atmospheric and oceanic properties averaged over cloudy regions for $SST = 28$–29 and 29–30 °C, respectively.

	$SST = 28$–29 °C	$SST = 29$–30 °C
Cloud amount (%)	85.6	41.8
Convective cloud amount (%)	6.1	3.2
Raining stratiform cloud amount (%)	25.3	6.0
Non-raining stratiform cloud amount (%)	54.2	32.6
SST (°C)	28.6	29.3
Surface net heat flux (W m^{-2})	−82.8	20.3
Surface latent heat flux (W m^{-2})	−158.2	−110.0
Surface solar radiative flux (W m^{-2})	157.7	205.3
IWP (mm)	0.34	0.20
LWP (mm)	0.33	0.32
Mass-weighted temperature (°C)	−25.7	−23.9
PW (mm)	54.2	53.9

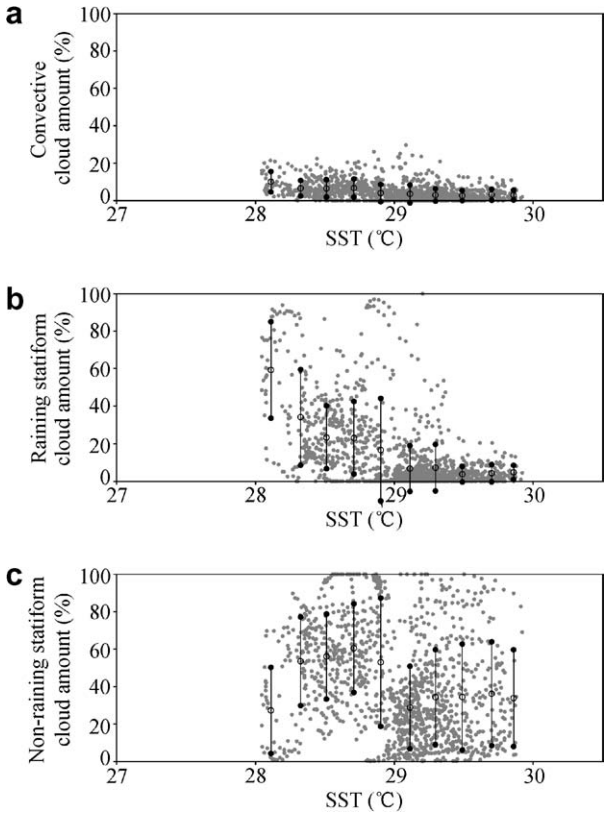

Fig. 3. Scatterplot of (a) convective, (b) raining stratiform, and (c) non-raining stratiform cloud amount versus SST (grey) and against SST binned at 0.2 °C intervals. The error bars indicate the standard deviations within each SST category.

amount and non-raining stratiform cloud amount are 65.8%, 54.9%, and 30.1%, respectively. The smallest RMS difference between cloud amount and non-raining stratiform cloud amount indicates that non-raining stratiform clouds are a major contributor to cloud amount. The mean convective, raining stratiform, and non-raining stratiform cloud amounts are 6.1%, 25.3%, and 54.2%, respectively, when SST is at 28–29 °C, whereas they are 3.2%, 6.0%, and 32.6%, respectively, when SST is at 29–30 °C (Table 1). The largest decrease in cloud amount is the raining stratiform cloud for the three types of clouds. This suggests that raining stratiform clouds are also a significant contributor to cloud amount when SST is lower, whereas they are not when SST is higher.

The atmosphere may affect the ocean through changing the surface fluxes. To explore the relation between the cloud amount and SST over cloudy regions, the surface net heat flux (sum of solar and IR radiative fluxes and sensible and latent heat fluxes; positive value when the flux goes into the ocean) as a function of SST was analyzed. The surface net heat flux showed larger positive values when SST was at 29–30 °C than those when SST was at 28–29 °C (Fig. 4a). The variation of surface net heat flux is mainly determined by the variation of surface solar radiative flux (Fig. 4b), since the change of surface latent heat flux (Fig. 4c) is much smaller than that of surface solar radiative flux. The difference (103.1 W m^{-2}) in mean surface net heat flux between high SST bin (29–30 °C) and low SST bin (28–29 °C) is determined by the differences in both mean surface solar radiative (47.6 W m^{-2}) and latent heat (48.2 W m^{-2}) fluxes (see Table 1).

Cloud amount decreases as surface solar radiative flux increases (Fig. 4d). Although the cloud amount shows a large fluctuation for certain solar flux, the linear correlation coefficient between cloud amount and surface solar flux is −0.13, which exceeds the 1% confidence level. Thus, the relation is statistically significant. The cloud hydrometeors are major players in atmospheric radiation budgets. Gao [40] in his equilibrium study with the 2D cloud-resolving model showed that ice clouds (or IWP) are a major absorber for solar radiation, whereas water clouds (or LWP) are a minor absorber. The major contributor to cloud amount is from non-raining stratiform clouds that dominated by the anvil clouds. Thus, the relation between IWP and surface solar radiative flux has been investigated. The result showed that surface solar radiative flux increased as IWP decreased (Fig. 4e). This suggests that small (large) amounts of ice clouds associated with small (large) cloud amounts reflect small (large) amounts of solar radiation back to the space and allow large (small) amounts of solar radiation reaching to the surface.

The results are summarized by averaging the simulation data for $SST = 28$–29 and 29–30 °C individually (Table 1). The small mean cloud amount (41.8%) is associated with the small mean IWP (0.20 mm) that reflects the small amount of solar radiation back to the space and allows the large mean amount of solar radiation reaching to the ocean (205.3 W m^{-2}), and getting a high SST (29.3 °C). The large mean cloud amount (85.6%) is associated with the large mean IWP (0.34 mm) that leads to the small mean amount of surface solar radiation (157.7 W m^{-2}), and getting a low SST (28.6 °C).

Considering that the only direct way in which the ocean affects the atmosphere is through surface sensible heat flux in the heat budget and surface evaporation flux in the water

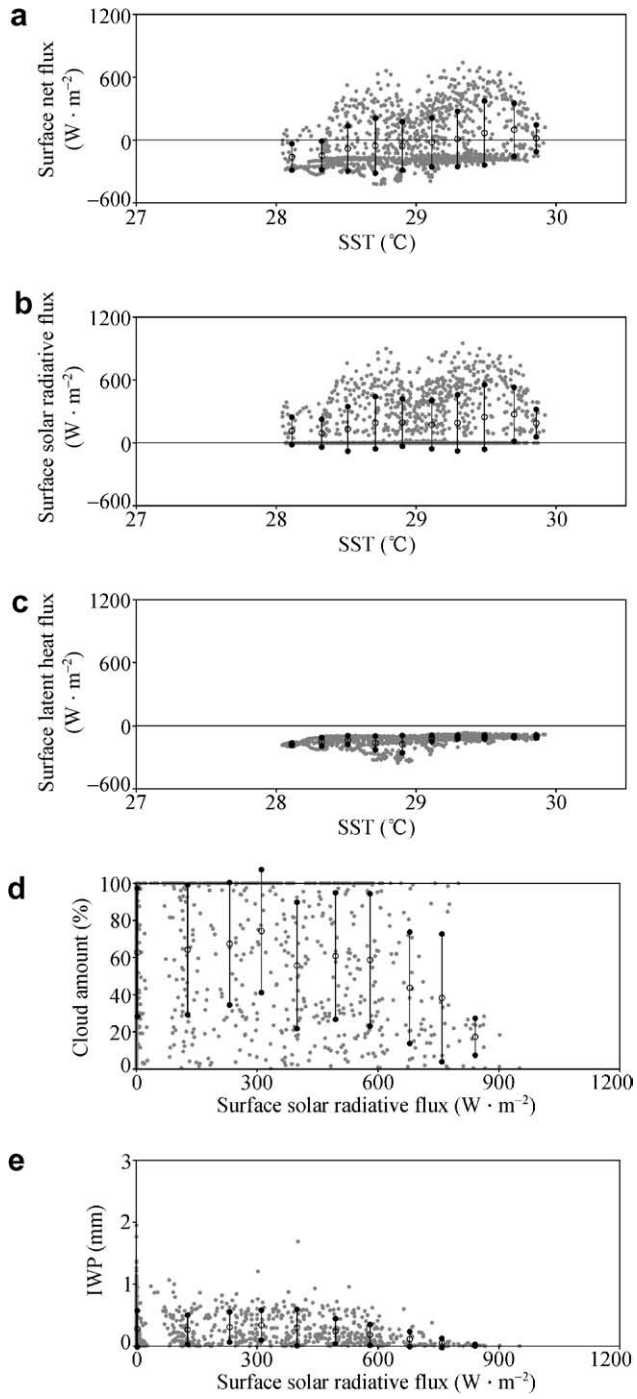

Fig. 4. Scatterplot of (a) surface net flux ($W\,m^{-2}$), (b) surface solar radiative flux, (c) surface latent heat flux versus SST (grey) and against SST binned at 0.2 °C intervals, (d) cloud amount and IWP versus surface solar radiative flux (grey) and against surface solar radiative flux binned at 30 $W\,m^{-2}$ intervals. The error bars indicate the standard deviations within each SST category in (a–c) and each surface solar radiative flux category in (d–e).

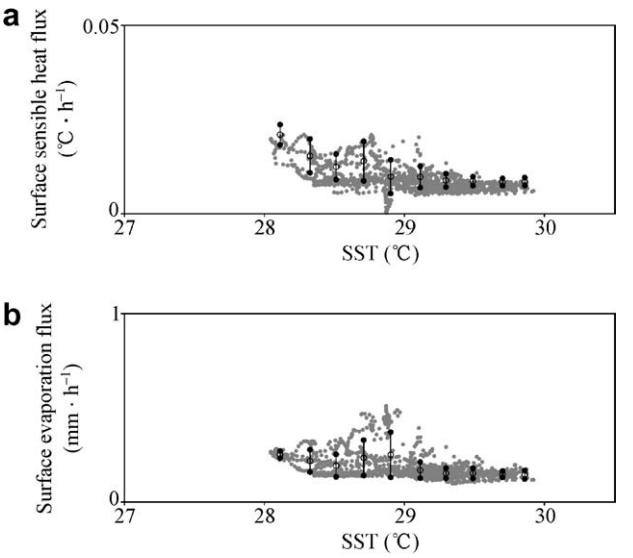

Fig. 5. Scatterplot of (a) surface sensible heat flux ($°C\,h^{-1}$) and (b) surface evaporation flux ($mm\,h^{-1}$) versus SST (grey) and against SST binned at 0.2 °C intervals. The error bars indicate the standard deviations within each SST category.

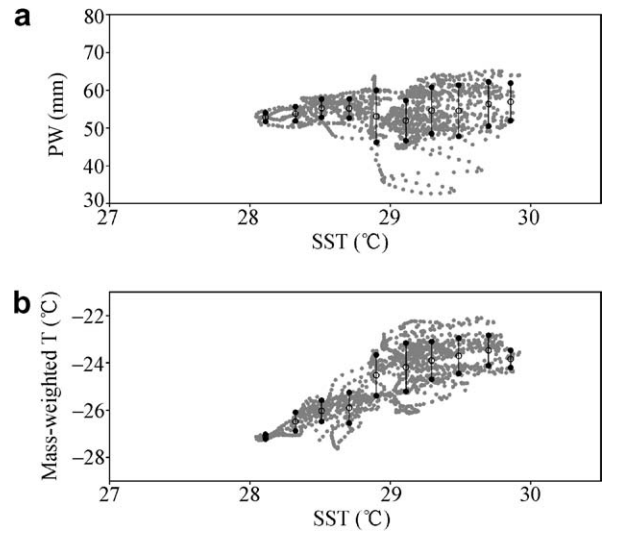

Fig. 6. Scatterplot of (a) PW and (b) mass-weighted temperature versus SST (grey) and against SST binned at 0.2 °C intervals. The error bars indicate the standard deviations within each SST category.

vapor budget, we plot the surface sensible heat flux versus SST and the surface evaporation flux versus SST as shown in Fig. 5. Precipitable water (PW) versus SST and mass-weighted temperature versus SST are plotted in Fig. 6, and IWP and LWP versus SST are plotted in Fig. 7. Both surface sensible heat and evaporation fluxes decrease as SST increases. Mass-weighted temperature increases with increasing SST, while PW may not be very sensitive to the change of SST. IWP decreases as SST increases, while LWP may not be sensitive to SST. Thus, oceanic processes do not have direct impacts on atmospheric heat and water vapor budgets. The negative correlation between the cloud amount and SST over cloudy regions calculated with hourly grid simulation data shows that the oceanic effects do not play an important role in determining the atmospheric variability.

A large mean IWP (0.34 mm) is associated with a cold atmosphere ($T = -25.7$ °C), whereas a small mean IWP

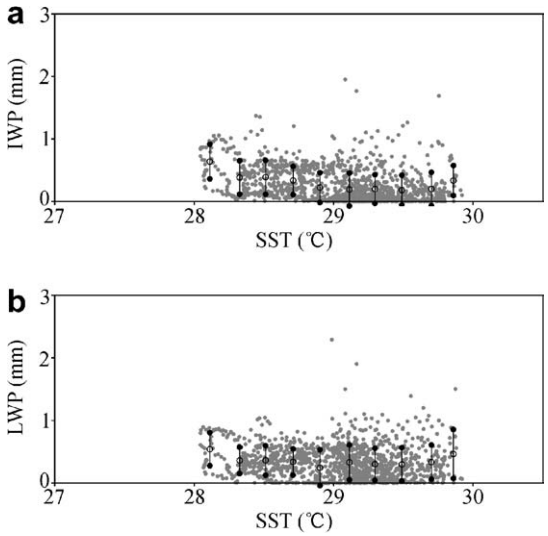

Fig. 7. Scatterplot of (a) IWP and (b) LWP versus SST (grey) and against SST binned at 0.2 °C intervals. The error bars indicate the standard deviations within each SST category.

(0.20 mm) is associated with a warm atmosphere ($T = -23.9$ °C) although both cold and warm atmospheres have similar mean amounts of PW, indicating that the air temperature may determine the IWP. Sui et al. [34] showed that the cold temperature reduces air capacity to hold atmospheric water vapor and thus leads to the increase of vapor condensation and depositions. Both cold and warm atmospheres have similar mean LWPs, suggesting that the water vapor may determine the LWP.

4. Conclusion

The relation between cloud amount and SST over Western Tropical Pacific cloudy regions has been examined based on the hourly data from a 2D coupled ocean–cloud resolving atmosphere simulation. The model is integrated for 50 days subject to forcing of large-scale vertical velocity and zonal wind derived and observed from TOGA COARE data. The analysis shows that the cloud amount decreases as the sea surface temperature increases. This negative correlation is similar to that found by Lindzen et al. [17].

The surface sensible heat and evaporation fluxes decrease as SST increases. The atmospheric temperature increases as SST increases, while the air water vapor is not sensitive to SST. These indicate that the ocean does not play an important role in determining the atmospheric heat and water vapor budgets. The large (small) IWP is associated with a cold (warm) atmosphere while both cold and warm atmospheres have similar amounts of water vapor. This suggests that the IWP depends on the air temperature. The air water vapor may determine the LWP, since both cold and warm atmospheres have similar amount of water vapor and similar LWP. Costa et al. [16] analyzed the sensitivity of cloud coverage to SST with cloud-resolving model simulations and argued that a positive feedback occurs between cloud coverage and SST in the transition from the marine stratocumulus to trade wind cumulus. Low (high) SST supports (destroys) stratiform clouds, increasing (reducing) the fractional cloud coverage, which further cools (warms) the ocean surface. Our coupled modeling study here does not support this feedback mechanism between cloud amount and SST due to the fact that ocean does not have an obvious effect on atmosphere. The surface solar radiative flux is the major component for surface net heat flux that determines the SST in our coupled modeling study. This is different from the results of cloud-resolving model experiments with different fixed SSTs conducted by Costa et al. [16] that the amount of solar radiation reaching the ocean surface is insensitive to imposed constant SST in the model.

The cold atmosphere produces a larger IWP and associated ice clouds occupy a larger area than the warm atmosphere does. The larger IWP with larger cloud amount allows less solar radiation getting into the ocean, which leads to a colder ocean surface than that produced by a smaller IWP with smaller cloud amounts. Thus, the negative correlation between the cloud amount and SST reflects the important atmospheric effects on the ocean. Note that the study uses hourly simulation data and the model with current spatial resolution may not properly simulate shallow cumulus clouds that may have effects of solar radiation and surface solar radiative flux, therefore it requests further studies. Since the forcing is from TOGA COARE, our results only show the air–sea coupling case over western Pacific warm pool. More experiments should be carried out over different climatic regimes and in different seasons to test the relation between cloud amount and SST.

Acknowledgements

This work was supported by the National Basic Research Program of China (Grant No. 2004CB418301), the Chinese Academy of Sciences (Grant No. KCL14014), the National Natural Sciences Foundation of China (Grant No.40433007) and the Knowledge Innovation Project of Chinese Academy of Sciences (No. IAP07214).

References

[1] Weller RA, Anderson SP. Surface meteorology and air–sea fluxes in the western equatorial Pacific warm pool during TOGA COARE. J Climate 1996;9:1959–90.
[2] Sui CH, Li X, Lau KM, et al. Multi-scale air–sea interaction during TOGA COARE. Mon Wea Rev 1997;125:448–62.
[3] Li X, Sui CH, Adamec D, et al. Impacts of precipitation in the upper ocean in the Western Pacific warm pool during TOGA COARE. J Geophys Res 1998;103:5347–59.
[4] Albrecht BA. Parameterization of trade-cumulus cloud amounts. J Atmos Sci 1981;38:97–105.
[5] Betts AK, Ridgway W. Climatic equilibrium of the atmospheric convective boundary layer over a tropical ocean. J Atmos Sci 1989;46:2621–41.

[6] Oreopoulos L, Davies R. Statistical dependence of albedo and cloud cover on sea surface temperature for two tropical marine stratocumulus regions. J Climate 1993;6:2434–47.
[7] Norris JR, Leory CB. Interannual variability in stratiform cloudiness and sea surface temperature. J Climate 1994;7:1915–25.
[8] Ramanathan V, Collins W. Thermodynamic regulation of ocean warming by cirrus clouds deduced from observations of the 1987 El Nino. Nature 1991;351:27–32.
[9] Arking A, Ziskin D. Relationship between clouds and sea surface temperature in the Western Tropical Pacific. J Climate 1994;7:988–1000.
[10] Bony S, Lau KM, Sud YC. Sea surface temperature and large-scale circulation influences on tropical greenhouse effect and cloud radiative forcing. J Climate 1997;10:2055–77.
[11] Rossow W, Schiffer R. ISCCP cloud data products. Bull Am Meteor Soc 1991;72:2–20.
[12] Susskind J, Piraino P, Rokke L, et al. Characteristics of TOVS Pathfinder Path A dataset. Bull Am Meoeor Soc 1997;78:1449–72.
[13] Reynolds RW, Smith TM. Improved global sea surface temperature analyses using optimum interpolation. J Climate 1994;7:929–48.
[14] Tompkins AM, Craig GC. Sensitivity of tropical convection to sea surface temperature in the absence of large-scale flow. J Climate 1999;12:462–76.
[15] Wu X, Moncrieff MW. Effects of sea surface temperature and large-scale dynamics on the thermodynamic equilibrium state and convection over the tropical western Pacific. J Geophys Res 1999;104:6093–100.
[16] Costa AA, Cotton WR, Walko RL, et al. SST sensitivities in mulltiday TOGA COARE cloud-resolving simulations. J Atmos Sci 2001;58:253–68.
[17] Lindzen RS, Chou MD, Hou AY. Does the Earth have an adaptive infrared iris?. Bull Am Meteor Soc 2001;82:417–32.
[18] Li X, Sui CH, Lau KM, et al. Effects of precipitation on ocean mixed-layer temperature and salinity as simulated in a 2-D coupled ocean–cloud resolving atmosphere model. J Meteor Soc Japan 2000;78:647–59.
[19] Gao S, Ping F, Li X. Cloud microphysical processes associated with the diurnal variations of tropical convection: a 2D cloud resolving modeling study. Meteor Atmos Phys 2006;91:9–16.
[20] Soong ST, Ogura Y. Response of tradewind cumuli to large-scale processes. J Atmos Sci 1980;37:2035–50.
[21] Soong ST, Tao WK. Response of deep tropical cumulus clouds to mesoscale processes. J Atmos Sci 1980;37:2016–34.
[22] Tao WK, Simpson J. The Goddard Cumulus Ensemble model. Part I: Model description. Terr Atmos Oceanic Sci 1993;4:35–72.
[23] Li X, Sui CH, Lau KM, et al. Large-scale forcing and cloud-radiation interaction in the tropical deep convective regime. J Atmos Sci 1999;56:3028–42.
[24] Lin YL, Farley RD, Orville HD. Bulk parameterization of the snow field in a cloud model. J Climate Appl Meteor 1983;22:1065–92.
[25] Rutledge SA, Hobbs PV. The mesoscale and microscale structure and organization of clouds and precipitation in midlatitude cyclones. Part VIII: a model for the "seeder–feeder" process in warm-frontal rainbands. J Atmos Sci 1983;40:1185–206.
[26] Rutledge SA, Hobbs PV. The mesoscale and microscale structure and organization of clouds and precipitation in midlatitude cyclones. Part XII: a diagnostic modeling study of precipitation development in narrow cold-frontal rainbands. J Atmos Sci 1984;41:2949–72.
[27] Tao WK, Simpson J, McCumber M. An ice-water saturation adjustment. Mon Wea Rev 1989;117:231–5.
[28] Krueger SK, Fu Q, Liou KN, et al. Improvement of an ice-phase microphysics parameterization for use in numerical simulations of tropical convection. J Appl Meteor 1995;34:281–7.
[29] Chou MD, Suarez MJ, Ho CH, et al. Parameterizations for cloud overlapping and shortwave single scattering properties for use in general circulation and cloud ensemble models. J Atmos Sci 1998;55:201–14.
[30] Chou MD, Kratz DP, Ridgway W. Infrared radiation parameterization in numerical climate models. J Climate 1991;4:424–37.
[31] Chou MD, Suarez MJ. An efficient thermal infrared radiation parameterization for use in general circulation model. In: NASA Tech Memo 104606, vol. 3. 1994. p. 85.
[32] Adamec D, Elsberry RL, Garwood RW, et al. An embedded mixed-layer ocean circulation model. Dyn Atmos Oceans 1981;6:69–96.
[33] Niiler PP, Kraus EB. One-dimensional models. In: Modeling and prediction of the upper layers of the ocean. New York: Pergamon; 1977. p. 43–172.
[34] Sui CH, Li X, Lau KM. Selective absorption of solar radiation and upper ocean temperature in the equatorial western Pacific. J Geophys Res 1998;103:10313–21.
[35] Sui CH, Lau KM, Takayabu Y, et al. Diurnal variations in tropical oceanic cumulus ensemble during TOGA COARE. J Atmos Sci 1997;54:639–55.
[36] Gao S, Li X. Cloud-resolving modeling of convective processes. Dordrecht: Springer; 2008, p. 206.
[37] Sui CH, Tsay CT, Li X. Convective stratiform rainfall separation by cloud content. J Geophys Res 2007;112:D14213.
[38] Tao WK, Simpson J, Sui CH, et al. Heating, moisture, and water budgets of tropical and midlatitude squall lines: comparisons and sensitivity to longwave radiation. J Atmos Sci 1993;50:673–90.
[39] Sui CH, Lau KM, Tao WK, et al. The tropical water and energy cycles in a cumulus ensemble model. Part I: equilibrium climate. J Atmos Sci 1994;51:711–28.
[40] Gao S. A cloud-resolving modeling study of cloud radiative effects on tropical equilibrium states. J Geophys Res 2007;113:D03108.